Improved constraints on ultralight axions using latest observations of the early and late Universe

Qianshuo Liu,[1,2] Chang Feng,[1,2,*] and Filipe B. Abdalla[1,2]
[1]Department of Astronomy, University of Science and Technology of China, Hefei 230026, China
[2]School of Astronomy and Space Science, University of Science and Technology of China, Hefei 230026, China

(Received 1 August 2025; accepted 15 January 2026; published 18 February 2026)

Ultralight axions (ULAs) are hypothetical particles which can behave like dark matter (DM) or dark energy (DE) depending on masses generated at the symmetry-breaking scale. It remains a mystery whether the ULAs can make up a fraction of DM or DE. Although theoretical predictions indicate that the ULAs may leave distinct imprints on cosmological signals, these signatures may exist in a broad spatial and temporal scales, and may be degenerate with the known effects of the standard model. The ULA signatures are extremely subtle and the observational evidence of the ULAs remain elusive. In this work, we infer the ULA properties using both the early and late universe observations from the cosmic microwave background (CMB) and baryon acoustic oscillations (BAO). We validate modeling of the ULA effects using the CMB and BAO mock data and perform different tests to cross-check the results. By analyzing the Planck 2018 CMB measurements and the BAO measurements from the Data Release 2 of Dark Energy Spectroscopic Instrument (DESI), we constrain the energy density fraction ratio of the ULAs to total dark matter Ω_a/Ω_d and obtain a new upper bound of Ω_a/Ω_d. Future CMB and BAO measurements will achieve unprecedented precision and will be crucial for understanding the nature of the ULAs.

DOI: 10.1103/df2p-1c8s

I. INTRODUCTION

Axions were initially introduced to solve the strong charge-parity problem [1] and may have profound cosmological and astrophysical implications at ultralow mass regime, where extremely long de Broglie wavelengths of the ultralight axions (ULAs) can leave unique imprints on cosmological and astrophysical observations, such as the cosmic microwave background (CMB), baryon acoustic oscillations (BAO) and spatial matter fluctuations.

The ULA can be described by a scalar field ϕ in a periodic potential $V(\phi) = m_a^2 f_a^2[1 - \cos(\phi/f_a)]$ where the ULA mass is m_a and the symmetry-breaking scale is f_a [2]. The scalar field can roll down the potential and start oscillating when it reaches the minimum, manifesting a dynamical nature. The evolution timescale of the scalar field is determined by its mass, and the scalar field with a mass of 10^{-27} eV can begin oscillations around the radiation-matter equality [3].

For masses larger than 10^{-27} eV, the ULAs begin oscillations in the very early universe and behave like dark matter (DM). The ULA can modify the epoch of matter-radiation equality and affect the CMB acoustic peaks. Also, the DM-like ULAs can leave unique suppression features on the matter fluctuations [3–5].

For masses lower than 10^{-27} eV, the ULAs begin oscillations in the late Universe so behave like dark energy (DE) accelerating the expansion of our Universe. The DE-like ULAs can change the distance to the last scattering surface, the decaying gravitational potential for the integrated Sachs-Wolfe (ISW) effect, and the structure growth in the late Universe. Thus, the locations of the CMB acoustic peaks can be shifted, the smearing effects of gravitational lensing can be adjusted, and the large-scale fluctuations can be altered. Also, the matter fluctuations may experience a global decrease due to an insufficient amount of growth time [4,5].

These ULA effects have been searched for and the energy density fraction ratio of the ULA (Ω_a) to total dark matter (Ω_d), i.e., $f_{ax} = \Omega_a/\Omega_d$ has been constrained by different observational datasets. A constraint of joint CMB measurements from Wilkinson Microwave Anisotropy Probe, Planck satellite, Atacama Cosmology Telescope and South Pole Telescope, and galaxy power spectrum measurements from the WiggleZ dark energy survey [6] is found to be $f_{ax} < 0.048$ in mass range 10^{-33} eV $< m_a < 10^{-25.5}$ eV [5]. The result is further improved to $f_{ax} < 0.019$ at $m_a = 10^{-28}$ eV with Planck 2018 data release [7]. By adding monopole and quadrupole moments of galaxy clustering measurements, the ULA fraction constraint is further pushed down to $f_{ax} < 0.014$ at $m_a = 10^{-28}$ eV [8]. With better sensitivities coming from Planck 2018 CMB

*Contact author: changfeng@ustc.edu.cn

data release and higher-order galaxy power spectra from Baryon Oscillation Spectroscopic Survey (BOSS) [9], an improved constraint is found to be $f_{ax} < 0.008$ at $m_a = 10^{-28}$ eV [10,11] and can be slightly higher at $f_{ax} < 0.011$ if an extended two-fluid model is adopted [11]. In addition, small-scale Lyman-α measurements yield a new limit $f_{ax} \sim$ 0.01-0.05 at a much higher mass $m_a = 10^{-25}$ eV [12]. Different from the fluctuations and distance measurements, a recent analysis shows that cluster number counts can also place an interesting limit $f_{ax} < 0.013$ at $m_a = 10^{-28}$ eV [13].

The ULA dark energy nature implies that it could be an evolving dark energy component. It is unclear if the recent evidence of dynamical dark energy (DDE) from the DESI data release 2 (DR2) can be partially accounted for by the ULA species [14]. In this work, we run a Bayesian analysis to infer the ULA fraction f_{ax} from the Planck 2018 CMB and DESI-DR2 datasets and infer the DDE properties in the presence of the ULA component. The achieved limits on the ULA fractions are mainly contributed by the DESI DR2 BAO measurements but the ULA physics implications in the context of the DDE is a new focus of this work and would be important for unveiling the nature of dark matter and dark energy.

II. DATASETS AND METHOD VALIDATIONS

There are multiple numerical implementations of the ULA physics, such as axionCAMB [5] and AxiCLASS [15]. In this work, we adopt axionCAMB as the baseline method to derive statistical properties of ULA physics. Effective fluid approximations adopted in the axionCAMB have been recently validated by exact solutions of the ULA fields [16].

We can describe the ULA evolution with a cosinelike potential $V(\phi) = m_a^2 f_a^2 [1 - \cos(\phi/f_a)]^n$ with $n = 1$, which can be approximated as $V(\phi) \sim (1/2) m_a^2 \phi^2$. The ULAs with potential $n > 1$ will become a radiation relic today [15]. The CMB power spectra with ULA physics can be calculated with the dynamical evolution of the ULA field included in the Boltzmann equation. We use axionCAMB to compute lensed power spectra for CMB observables, time-dependent Hubble parameter and comoving distance for the BAO observables.

A. CMB and BAO measurements

We use Planck 2018 CMB power spectra which contain C_ℓ^{TT} within the multipole range $30 \le \ell \le 2508$, and C_ℓ^{EE} and C_ℓ^{TE} within the multipole range $30 \le \ell \le 1996$ [17]. In addition, we include the large-scale power spectra C_ℓ^{TT} and C_ℓ^{EE} at $2 \le \ell \le 29$. We do not include the Planck lensing measurement since it can only negligibly affect the limits on the ULA fractions. We use the Planck released likelihood function Plik to compute $\mathcal{L}_{\rm CMB}(\hat{d}_{\rm CMB}|\theta)$ [17]. Here $\hat{d}_{\rm CMB}$ refers to the measured CMB power spectra and θ denotes the cosmological parameters.

For the distance measurements, both the angle-averaged (D_V/r_d) and anisotropic $(D_H/r_d,\ D_M/r_d)$ BAO measurements at seven redshifts are released by DESI [14]. Here, $D_{i\in V,H,M}$ and r_d are comoving distances and sound horizon. Especially, to account for different correlations of the transverse and perpendicular BAO measurements, correlation coefficients are introduced in the covariance matrix for the likelihood function $\mathcal{L}_{\rm BAO}$ of the BAO

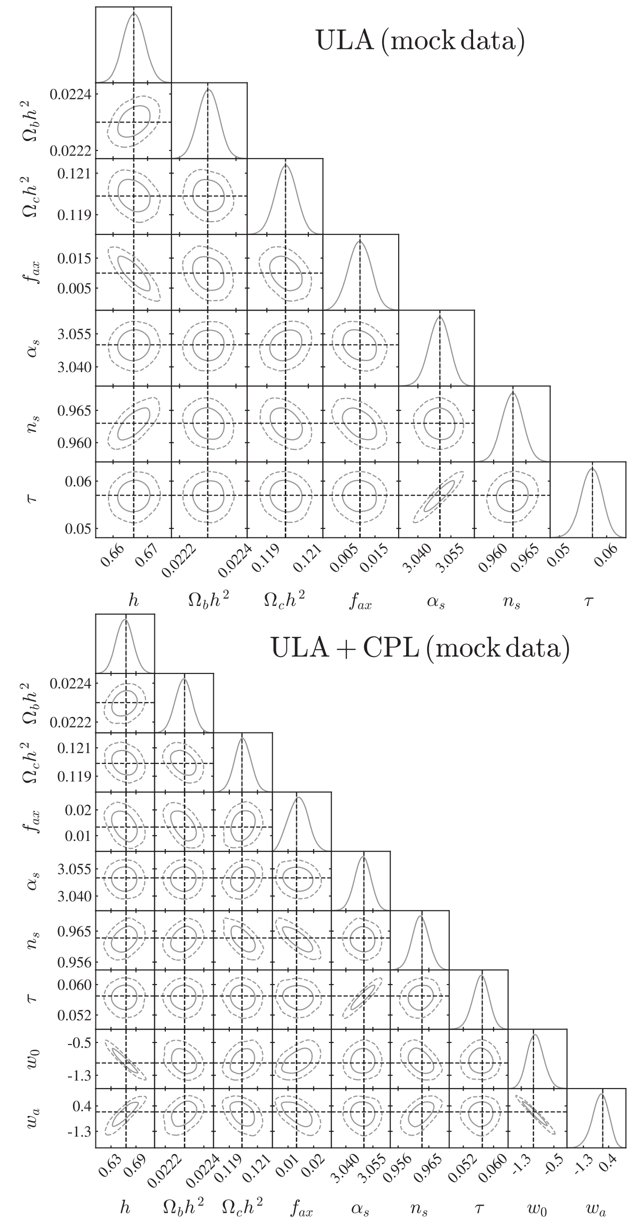

FIG. 1. Parameter inference from CMB and BAO mock datasets. In this test, we generate the mock data assuming an ULA fraction $\Omega_a/\Omega_d = 0.01$ at a representative mass $m_a = 10^{-28}$ eV. The inferred contours are consistent with the fiducial values, verifying that the Markov chain Monte Carlo analysis can fully recover the input cosmological parameters for the ULA masses considered in this work. Here, $\alpha_s = \ln(10^{10} A_s)$.

measurements. Posterior distribution functions (PDFs) of the cosmological parameters are thus inferred from $\mathcal{P}(\theta|\hat{d}) \sim \mathcal{L}_{\mathrm{CMB}}(\hat{d}|\theta)\mathcal{L}_{\mathrm{BAO}}(\hat{d}|\theta)\pi(\theta)$ where $\pi(\theta)$ are parameter priors.

B. Validations with mock CMB and BAO datasets

In this work, two scenarios have been tested. One is the Λ cold dark matter (ΛCDM) model with ULA physics and is referred to as `ULA`. Another one is referred to as `ULA+CPL` which is a combination of the ULA model and the Chevallier-Polarski-Linder (CPL) [18,19] model described as $w(a) = w_0 + w_a(1 - a)$ where w_0 and w_a are two free parameters and a is the cosmological scale factor.

We generated the mock datasets for the CMB power spectra and the BAO measurements assuming fiducial cosmological models with known ULA signals which are simulated with two ULA fractions at $f_{ax} = 0.01$ and $f_{ax} = 10^{-4}$ representing a nonzero ULA detection and a null detection scenarios, respectively. We assume a futuristic cosmic-variance-limited CMB survey with a fullsky coverage and noiseless observations and simulate the corresponding C_ℓ^{TT}, C_ℓ^{EE}, and C_ℓ^{TE} power spectra at the same ℓ range as the Planck data. We theoretically calculate the different distance ratios D_V/r_d, D_M/r_d, and D_H/r_d at the seven redshifts where the DESI BAO measurements are made, while directly taking the covariance matrices and correlation coefficients from the DESI-DR2 distance measurements. Thus, there are four types of mock datasets used for the validations, i.e., `ULA` ($f_{ax} = 0.01$), `ULA` ($f_{ax} = 10^{-4}$), `ULA+CPL` ($f_{ax} = 0.01$), and `ULA+CPL` ($f_{ax} = 10^{-4}$). The test results in Fig. 1 demonstrate that the reconstructed PDFs of the cosmological parameters consistently peak at the fiducial values at the ULA mass $m_a = 10^{-28}$ eV. Similar validations have been performed for other ULA masses and the reconstructed PDFs are also consistent with the theoretical models.

We also investigated the prior impact on the parameters. Specifically, we tested the inference of the ULA fraction f_{ax} with a uniform prior on $\log_{10}(f_{ax})$. The inferred ULA fraction with such a prior is consistent with the input value if there is a nonzero ULA component. However, the inferred upper bound on the ULA fraction with a uniform prior on $\log_{10}(f_{ax})$ is slightly smaller than the one with a uniform prior on f_{ax} directly if no ULA is assumed because the uniform prior on $\log_{10}(f_{ax})$ allows a dense population at extremely small value of f_{ax}. As a conservative approach, we adopt the uniform prior on the ULA fraction f_{ax} as our benchmark test.

III. DATA ANALYSIS RESULTS AND DISCUSSIONS

We run the data analyses using the Planck 2018 CMB power spectra and DESI-DR2 BAO measurements and sample the posterior distributions from $\mathcal{P}(\theta|\hat{d}) \sim \mathcal{L}_{\mathrm{CMB}}(\hat{d}|\theta)\mathcal{L}_{\mathrm{BAO}}(\hat{d}|\theta)\pi(\theta)$ within the ULA mass range $10^{-31} < m_a < 10^{-27}$ eV. As seen from Fig. 2, we achieve a 0.7% upper bound on the ULA fraction at 10^{-28} eV. This is the most stringent constraint on the ULA fraction in the mass window within $10^{-31} < m_a < 10^{-27}$ eV so far. The detailed PDFs for all the parameters are shown in Fig. 3.

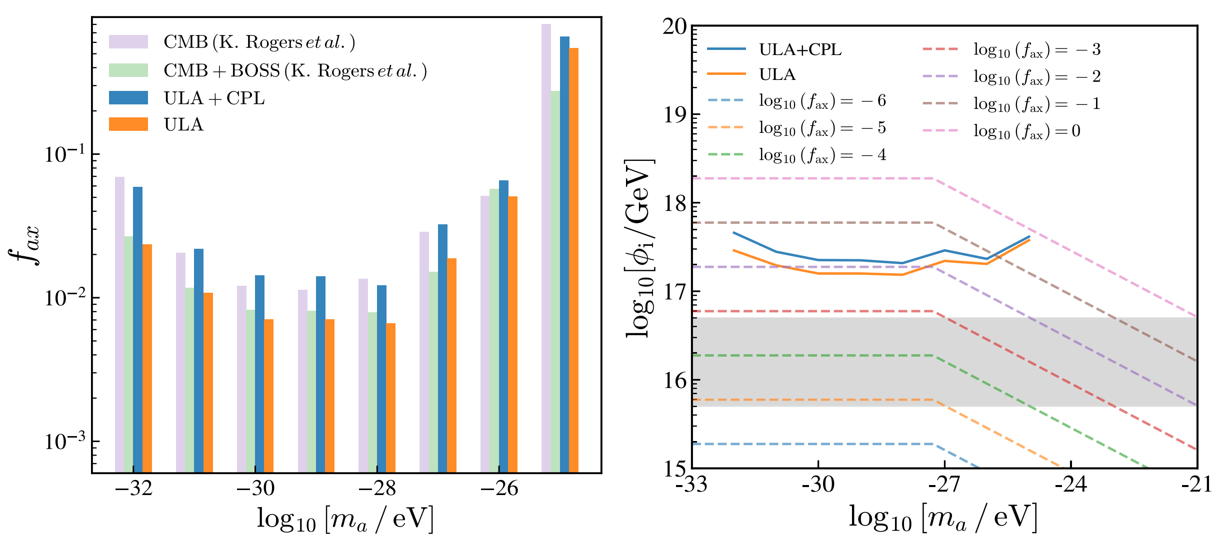

FIG. 2. (Left) 95% CL upper bounds on the ULA energy density fraction $f_{ax} = \Omega_a/\Omega_d$ across a range of masses. Results are shown for both `ULA`-only (orange) and `ULA+CPL` (blue) scenarios. The colored bands refer to the 95% upper bounds. The upper bounds from Planck + BOSS [10] are also shown for comparison. (Right) The inferred symmetry-breaking scale from the ULA energy density fractions. We use the Ω_a-ϕ_i relation derived in [5] to estimate the initial values of the ULA field ϕ_i which is related to the symmetry-break scale f_a by $\phi_i = \theta_i f_a$ with the initial misalignment angle θ_i being order of unity. The shaded region is the GUT energy scale between $10^{15.5} < f_a < 10^{16.5}$ GeV.

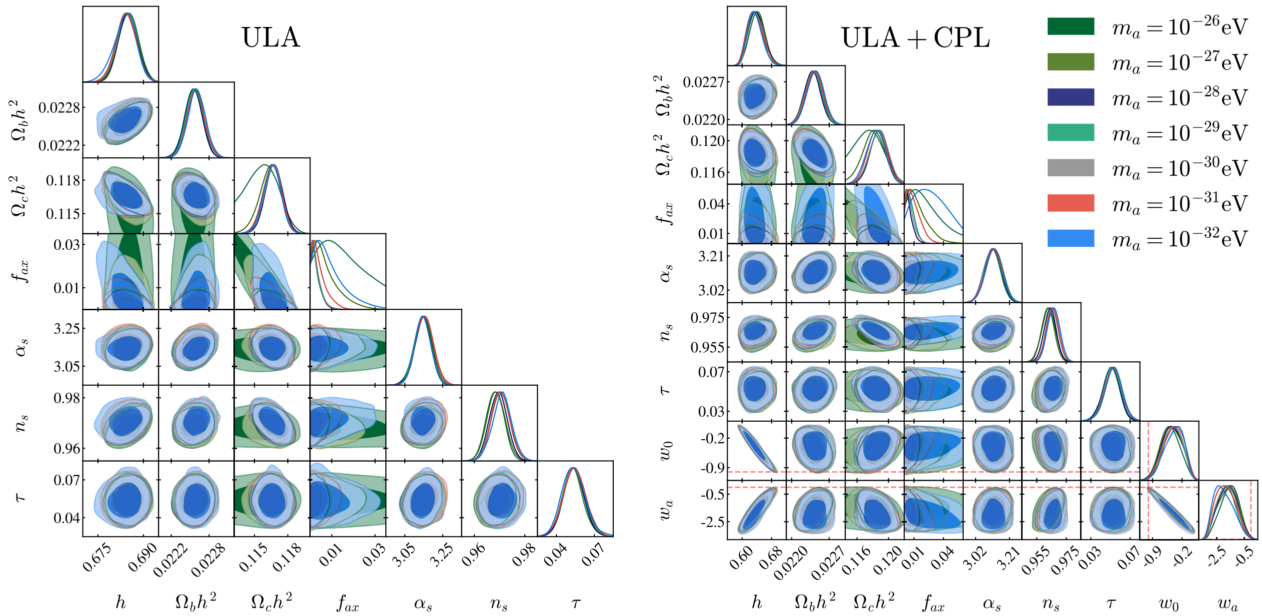

FIG. 3. Reconstructed PDFs of cosmological parameters from Planck 2018 CMB and DESI-DR2 BAO data. Two models are considered in this work: the ULA-only model (left) and the ULA+CPL model (right). The red dashed lines in the right panel denote the ΛCDM predictions.

We also list a few selected upper bounds on the ULA fractions in Table I.

While the inferred ULA fractions remain tightly constrained, we observe mild degeneracies between f_{ax} and cosmological parameters such as the spectral index n_s and amplitude A_s of the primordial curvature perturbation, the optical depth τ, and DM energy density fraction $\Omega_c h^2$. These arise because the ULA component can affect both the amplitudes and locations of the acoustic peaks of the CMB power spectra by either shifting the matter-radiation equality epoch when it is DM-like or accelerating the expansion history when it is DE-like. Moreover, the ISW effects constrained by the Planck low-ℓ data can further contribute to these correlations. However, the posterior distributions remain stable, indicating that the constraints are robust against these correlations. Although there are different levels of degeneracies among the parameters, both the one-dimensional posterior distribution functions and the upper bounds for the ULA fraction f_{ax} are derived by marginalizing other cosmological parameters, so the parameter correlations have been taken into account.

TABLE I. Upper bounds on the ULA fractions in the literature.

Upper bounds	ULA masses	References
$f_{ax} < 0.048$	$10^{-33} < m_a < 10^{-25.5}$ eV	[5]
$f_{ax} < 0.019$	$m_a = 10^{-28}$ eV	[7]
$f_{ax} < 0.014$	$m_a = 10^{-28}$ eV	[8]
$f_{ax} < 0.008$	$m_a = 10^{-28}$ eV	[10]
$f_{ax} \sim 0.01 - 0.05$	$m_a = 10^{-25}$ eV	[12]
$f_{ax} < 0.012$	$m_a = 10^{-27}$ eV	[13]
$f_{ax} < 0.007$	$m_a = 10^{-28}$ eV	This work

Interestingly, the right panel of Fig. 2 indicates that the current limit on the symmetry-breaking energy scale f_a is roughly an order of magnitude higher than the energy scale of the grand unified theory (GUT) in the mass range $10^{-30} < m_a < 10^{-28}$ eV, assuming that the initial misalignment angle θ_i is order of unity. We note that the upper bounds in the right panel of Fig. 2 are directly estimated for the initial field values ϕ_i, thus, are not affected by theoretical uncertainties of the parameter θ_i. However, the initial field values ϕ_i estimated for the GUT scales may be affected since they are scaled by the misalignment angle, i.e., $\phi_i = \theta_i f_a$ for given symmetry-breaking scales f_a. Given the fact that the initial misalignment angle is within the range of $0 < \theta_i < \pi$, the maximum value $\theta_i = \pi$, which is order of unity, corresponds to upper bounds on the initial field values of the GUT scales. The joint constraints from future CMB and BAO may be able to approach the GUT scale and the ULA signatures can be a smoking gun of the GUT physics.

Figure 4 shows that the constraints on the w_0-w_a parameter space are slightly changed by including the ULA component which also has an evolving nature. This result implies that the ULA impact on the DDE maybe negligible given its ultralow fraction. We note that this result is obtained with varying all nuisance parameters and if only an overall calibration parameter is assumed, the contours become consistent with the DESI result. Meanwhile, limited by the low fraction of f_{ax}, the ULAs do not change the constraints on the matter fraction

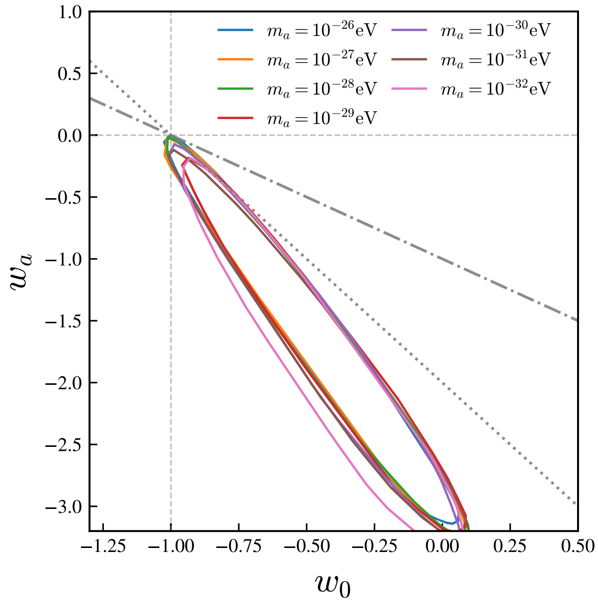

FIG. 4. Constraints on the w_0, w_a parameters from the ULA +CPL model. The 95% confidence levels do not show as a strong tension as the model with CPL-only. The vertical and horizontal dashed lines represent the ΛCDM model. The tilted dot-dashed line corresponds to the constraint $1 + w_0 + w_a = 0$ and the tilted dotted line is the constraint at $z = 1$ when $w_0 + (1 - a)w_a = -1$, i.e., $1 + w_0 + w_a/2 = 0$.

and the sound horizon, as seen from Fig. 5 where the difference is mainly driven by the dominant CPL model.

The ULA is actually a quintessence field with an equation of state w satisfying $-1 < w < 0$, so it cannot resolve the issue with phantom crossing that requires $w < -1$ [20] around $z \sim 0.4$ [14]. This limitation is not just technical but fundamental since the ULAs are confined to quintessencelike behavior as minimally coupled scalar fields with canonical kinetic terms, and cannot cross the so-called phantom divide [20]. Our results indicate that including ULAs can help reduce the statistical tension between ΛCDM and DDE models. This reduction should be viewed primarily as an effective degeneracy rather than a fundamental physical resolution, and its precise impact depends on the mass of the ULA considered. When marginalizing over axion masses, the overall effect is a net improvement, though individual fixed-mass cases may show varying levels of consistency with ΛCDM. The degree of mitigation ultimately depends on the precision of the data and the statistical significance of any deviation from $w = -1$. Should future surveys confirm phantomlike evolution with increasing confidence, models beyond single scalar fields, such as noncanonical fields [21], nonminimal couplings [22] and modified gravity theories [23], would be necessary to fully explain the observations.

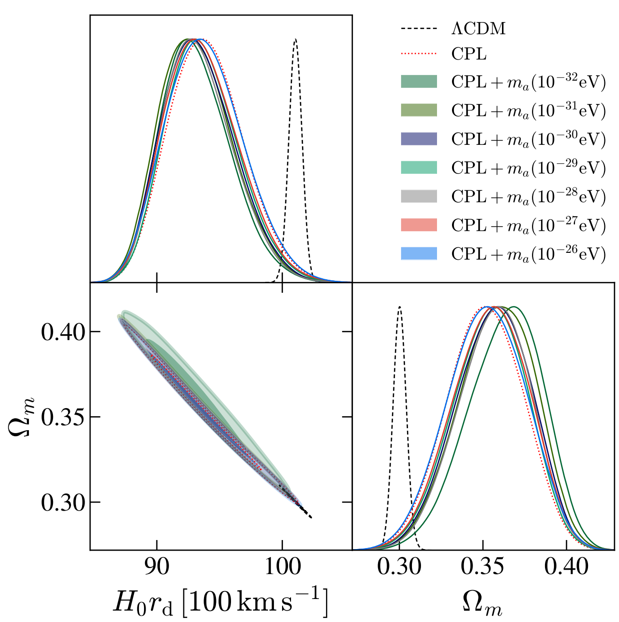

FIG. 5. Constraints on the $H_0 r_d$ and Ω_m parameters from different models. The constraint from the ULA-only model is consistent with the ΛCDM model and the main difference is driven by the inclusion of the CPL model.

In addition, in Sec. II, we only consider the potential with $n = 1$ but do not study the models with $n > 1$ [15]. The models with $n > 1$ behave like early dark energy (EDE) which mainly affects the radiation-dominated epoch and behaves like radiation in the late Universe. A recent analysis has shown that the inclusion of the EDE scenario can also reduce the preference for the dynamical dark energy and alleviate the Hubble tension [24]. The discussions in this work are only focused on the $n = 1$ cosine potential since the models with $n > 1$ behave like radiation and can not explain the nature of dynamical dark energy from the theoretical perspective. Therefore, the results should not be directly generalized to a broader class of axionlike models without detailed calculations.

The CMB power spectra released by Planck are derived from the foreground separated maps and contain different foreground residuals which may not be negligible to the ULA-induced CMB signatures. Specifically, these residuals consist of cosmic infrared background, thermal and kinetic Sunyaev-Zel'dovich (tSZ/kSZ) effects, residual Galactic foreground polarization, as well as instrumental effects such as calibrations.

We assigned different parameters to these residuals and marginalized all of these nuisance parameters for the inference of the cosmological parameters. These nuisance parameters included in the Plik package [17] are associated with either uniform or Gaussian priors, which are also included in the Bayesian analysis discussed in Sec. II.

To validate the CMB and BAO likelihood functions, we ran an analysis with the ΛCDM + CPL model and with all the nuisance parameters included. The inferred parameters are consistent with the ones using Cobaya [25].

We also ran the analysis with Planck likelihood package Plik_lite which only assumes a Gaussian prior on a single

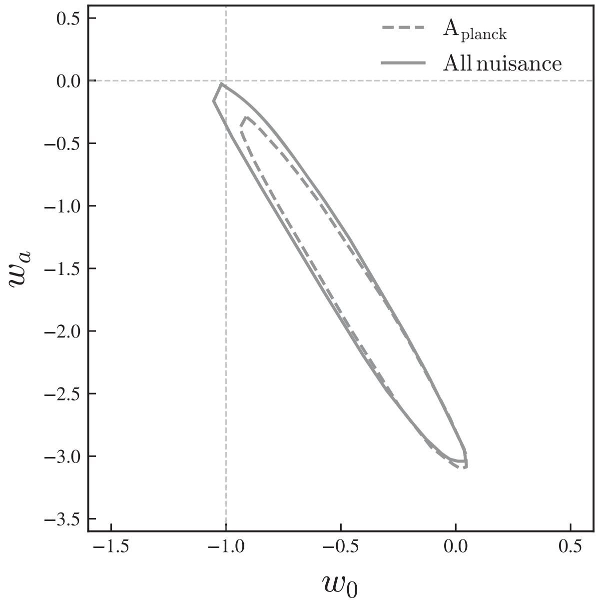

FIG. 6. The impact of nuisance parameters on the CPL model. We compare the inference of the CPL model under the assumptions of different nuisance parameters. The scenario with a single $A_{\rm Planck}$ parameter is consistent with the result in [14], while the deviation from the dark energy model with a cosmological constant is reduced as more nuisance parameters are included.

polarization calibration factor $A_{\rm Planck}$ while fixing other nuisance parameters as implemented in [10], our result is the same as the one in [14], as shown in Fig. 6.

IV. CONCLUSIONS

By jointly analyzing the Planck 2018 CMB data and seven BAO measurements from DESI data release 2, we obtain an improved constraints on the ULA fractions in the mass range 10^{-30} eV $< m_a < 10^{-28}$ eV. Also, the inferred w_0-w_a parameters show negligible impact from the ULA component under different assumptions for nuisance parameters.

The next-generation CMB polarization experiments will obtain high sensitivity datasets [26–28], and more precise and independent BAO measurements will also be obtained at both optical [29] and radio wavelengths [30]. The enormous constraining power of the future joint datasets may shed light on the nature of dark energy and find evidence of the ULA signatures.

All of these constraints presented in this work are obtained from the gravitational effects of the ULAs which may also leave interesting signatures through other mechanisms. The ULAs may be coupled to the electromagnetic field and generate a cosmological rotation effect [31,32] that can be precisely measured by the next-generation CMB polarization experiments. In addition, the ULAs can power the isocurvature perturbations [33] and the CMB polarization may place new limits on the ULA physics. Moreover, high precision matter clustering measurements [29] at different wavelengths can significantly break the degeneracies among cosmological parameters so the ULA signatures can be better constrained by a multitracer dataset in the future.

ACKNOWLEDGMENTS

This work is supported by the starting grant from the University of Science and Technology of China under Grant No. KY2030000148. F. B. A. acknowledges the support of the CAS. We acknowledge the use of the axionCAMB [5], EMCEE [34] packages.

DATA AVAILABILITY

The data that support the findings of this article are openly available [14,17].

[1] R. D. Peccei and H. R. Quinn, *CP* conservation in the presence of pseudoparticles, Phys. Rev. Lett. **38**, 1440 (1977).
[2] D. J. E. Marsh, Axion cosmology, Phys. Rep. **643**, 1 (2016).
[3] D. J. E. Marsh and P. G. Ferreira, Ultralight scalar fields and the growth of structure in the Universe, Phys. Rev. D **82**, 103528 (2010).
[4] D. J. E. Marsh, E. Macaulay, M. Trebitsch, and P. G. Ferreira, Ultralight axions: Degeneracies with massive neutrinos and forecasts for future cosmological observations, Phys. Rev. D **85**, 103514 (2012).
[5] R. Hlozek, D. Grin, D. J. E. Marsh, and P. G. Ferreira, A search for ultralight axions using precision cosmological data, Phys. Rev. D **91**, 103512 (2015).
[6] M. J. Drinkwater *et al.*, The WiggleZ dark energy survey: Survey design and first data release, Mon. Not. R. Astron. Soc. **401**, 1429 (2010).
[7] R. Hložek, D. J. E. Marsh, and D. Grin, Using the full power of the cosmic microwave background to probe axion dark matter, Mon. Not. R. Astron. Soc. **476**, 3063 (2018).
[8] A. Laguë, J. R. Bond, R. Hložek, K. K. Rogers, D. J. E. Marsh, and D. Grin, Constraining ultralight axions with galaxy surveys, J. Cosmol. Astropart. Phys. 01 (2022) 049.
[9] K. S. Dawson *et al.*, The Baryon oscillation spectroscopic survey of SDSS-III, Astron. J. **145**, 10 (2013).
[10] K. K. Rogers, R. Hložek, A. Laguë, M. M. Ivanov, O. H. E. Philcox, G. Cabass, K. Akitsu, and D. J. E. Marsh, Ultralight axions and the S_8 tension: Joint constraints from the

cosmic microwave background and galaxy clustering, J. Cosmol. Astropart. Phys. 06 (2023) 023.

[11] F. Verdiani, E. Castorina, E. Salvioni, and E. Sefusatti, The effective field theory of large scale structure for mixed dark matter scenarios, arXiv:2507.08792.

[12] K. K. Rogers and V. Poulin, 5σ tension between Planck cosmic microwave background and eBOSS Lyman-alpha forest and constraints on physics beyond ΛCDM, Phys. Rev. Res. **7**, L012018 (2025).

[13] S. Zelmer *et al.*, Constraints on ultra-light axion dark matter through galaxy cluster number counts, Astron. Astrophys. **704**, A346 (2025).

[14] M. Abdul-Karim *et al.* (DESI Collaboration), DESI DR2 results II: Measurements of baryon acoustic oscillations and cosmological constraints, Phys. Rev. D **112**, 083515 (2025).

[15] V. Poulin, T. L. Smith, D. Grin, T. Karwal, and M. Kamionkowski, Cosmological implications of ultralight axionlike fields, Phys. Rev. D **98**, 083525 (2018).

[16] R. Liu, W. Hu, and D. Grin, Accurate method for ultralight axion CMB and matter power spectra, Phys. Rev. D **112**, 023513 (2025).

[17] N. Aghanim *et al.* (Planck Collaboration), Planck 2018 results. V. CMB power spectra and likelihoods, Astron. Astrophys. **641**, A5 (2020).

[18] M. Chevallier and D. Polarski, Accelerating universes with scaling dark matter, Int. J. Mod. Phys. D **10**, 213 (2001).

[19] E. V. Linder, Exploring the expansion history of the universe, Phys. Rev. Lett. **90**, 091301 (2003).

[20] W. Hu, Crossing the phantom divide: Dark energy internal degrees of freedom, Phys. Rev. D **71**, 047301 (2005).

[21] C. Armendariz-Picon, V. Mukhanov, and P. J. Steinhardt, Essentials of k-essence, Phys. Rev. D **63**, 103510 (2001).

[22] W. J. Wolf, C. García-García, T. Anton, and P. G. Ferreira, Assessing cosmological evidence for non-minimal coupling, Phys. Rev. Lett. **135**, 081001 (2025).

[23] G. Ye, M. Martinelli, B. Hu, and A. Silvestri, Hints of nonminimally coupled gravity in DESI 2024 baryon acoustic oscillation measurements, Phys. Rev. Lett. **134**, 181002 (2025).

[24] Y.-H. Pang, X. Zhang, and Q.-G. Huang, The impact of the Hubble tension on the evidence for dynamical dark energy, Sci. China Phys. Mech. Astron. **68**, 280410 (2025).

[25] J. Torrado and A. Lewis, Cobaya: Code for Bayesian analysis of hierarchical physical models, J. Cosmol. Astropart. Phys. 05 (2021) 057.

[26] P. Ade *et al.*, The simons observatory: Science goals and forecasts, J. Cosmol. Astropart. Phys. 02 (2019) 056.

[27] S. Hanany *et al.*, PICO: Probe of inflation and cosmic origins, arXiv:1902.10541.

[28] A. Suzuki *et al.*, The LiteBIRD satellite mission: Sub-Kelvin instrument, J. Low Temp. Phys. **193**, 1048 (2018).

[29] Ž. Ivezić *et al.*, LSST: From science drivers to reference design and anticipated data products, Astrophys. J. **873**, 111 (2019).

[30] F. B. Abdalla, P. Bull, S. Camera, A. Benoit-Lévy, B. Joachimi, D. Kirk, H. R. Kloeckner, R. Maartens, A. Raccanelli, M. G. Santos, and G. B. Zhao, Cosmology from HI galaxy surveys with the SKA, in *Advancing Astrophysics with the Square Kilometre Array (AASKA14)* (2015), p. 17, arXiv:1501.04035.

[31] S. M. Carroll, G. B. Field, and R. Jackiw, Limits on a Lorentz- and parity-violating modification of electrodynamics, Phys. Rev. D **41**, 1231 (1990).

[32] E. Komatsu, New physics from the polarized light of the cosmic microwave background, Nat. Rev. Phys. **4**, 452 (2022).

[33] D. J. E. Marsh, D. Grin, R. Hlozek, and P. G. Ferreira, Tensor interpretation of bicep2 results severely constrains axion dark matter, Phys. Rev. Lett. **113**, 011801 (2014).

[34] D. Foreman-Mackey, D. W. Hogg, D. Lang, and J. Goodman, EMCEE: The MCMC Hammer, Publ. Astron. Soc. Pac. **125**, 306 (2013).